DOI: 10.1002/cphc.200900220

Single-Molecule Mechanical Unfolding of Amyloidogenic β_2-Microglobulin: The Force-Spectroscopy Approach

B. Sorce,[a] S. Sabella,[a] M. Sandal,[b] B. Samorì,[b] A. Santino,[c] R. Cingolani,[a] R. Rinaldi,[a, d] and P. P. Pompa*[a]

Over the past two decades, remarkable developments and refinements in single-molecule force spectroscopy (SMFS) techniques have been achieved, thus providing new investigation tools for biophysical and biological research. The potential of these techniques is demonstrated by the rapidly growing number of applications and reports,[1–3] and by the fact that these once cutting-edge techniques are currently becoming more reliable and precise. In a classical SMFS experiment (Figure 1 A), the cantilever tip is pressed onto a layer of proteins, immobilized on a substrate, followed by the extension of the protein molecules through the retraction of the piezoelectric positioner. Such an approach allows the measurement of the forces required to unfold protein domains, with piconewton sensitivity, and of the consequent changes of the protein length, with angstrom resolution. The technique acts directly on the protein molecule (that is maintained under physiological conditions), leaving its environment unchanged. SMFS is capable to monitor a variety of interactions between the stylus tip and the sample. However, upon interaction of the cantilever tip with the protein layer and the subsequent withdrawal of the piezoelectric positioner, many protein molecules interacting with the tip exert a force that bends the cantilever. Hence, the early part of the force-extension curve is frequently characterized by large fluctuations in force. This typically poses two difficulties in the interpretation of force-extension curves. First, the forces involved in the extension of short molecules may be masked by the noise caused by such nonspecific interactions. Second, almost all experiments show force peaks reflecting such nonspecific interactions, so that a means is required to differentiate true unfolding events from spurious interactions. The solution to this problem was found in molecular biology.[4] By ligating multiple copies of the cDNA encoding a specific

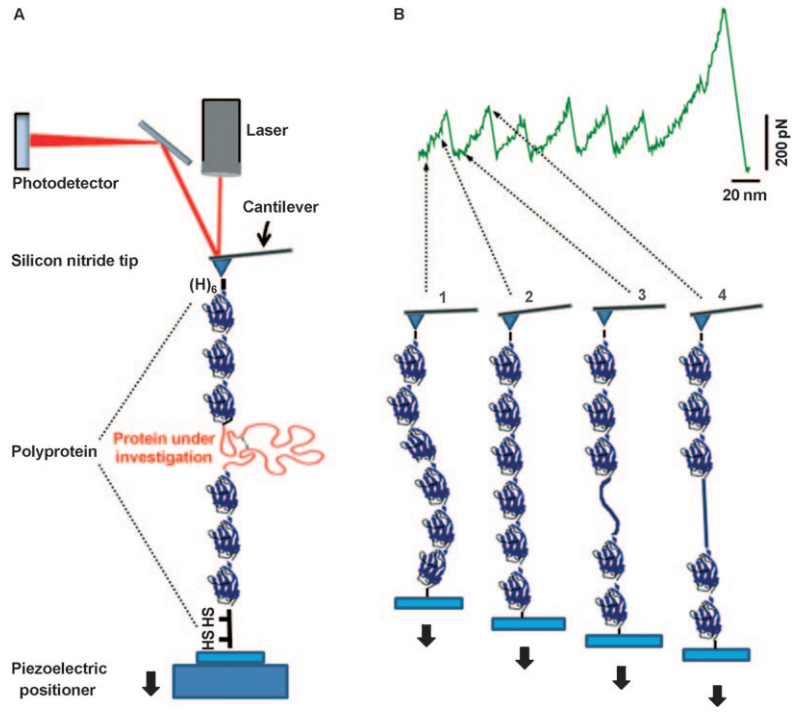

Figure 1. Schematic representation of a typical SMFS experiment on a polyprotein. A) The tip of the cantilever is brought into contact with proteins covalently immobilized onto a substrate, followed by the retraction of the piezoelectric positioner. The interaction of the tip with the proteins results in the bending of the cantilever. B) The stretching of the reference modules (such as I27) produces force-extension curves with a characteristic saw-tooth pattern. The individual saw-tooth peaks correspond to the sequential unraveling of individual domains in the reference multimodular protein. The unfolding force is a measure of the mechanical stability of the protein domains. As the piezoelectric positioner moves away (from step 1 to step 2), the protein generates a force on tip. After the unfolding of a specific domain, the length of the protein increases and the force acting on the cantilever is relaxed (step 3). Then, further extension results again in an increase of the force (step 4). The last peak in the force-extension curve represents the extension of the fully unfolded multimodular protein before its detachment from the tip or the substrate.

[a] *B. Sorce,[+] Dr. S. Sabella,[+] Prof. R. Cingolani, Prof. R. Rinaldi, Dr. P. P. Pompa*
National Nanotechnology Laboratory of INFM-CNR
Italian Institute of Technology (IIT)
Via Arnesano 16, 73100 Lecce (Italy)
Fax: (+39) 0832-298180
http://www.nnl.it
E-mail: piero.pompa@unile.it

[b] *Dr. M. Sandal, Prof. B. Samorì*
Department of Biochemistry "G. Moruzzi"
University of Bologna
Via Irnerio 48, 40126 Bologna (Italy)

[c] *Dr. A. Santino*
Institute of Sciences of Food Production C.N.R. Section of Lecce
Via Monteroni, 73100, Lecce (Italy)

[d] *Prof. R. Rinaldi*
University of Salento, Scuola Superiore ISUFI
73100 Lecce (Italy)

[+] *These authors contributed equally to this work*

protein domain and expressing the resultant gene in bacteria, it is possible to produce polyproteins consisting of multiple copies of a single protein. Unlike native modular proteins, polyproteins have a perfectly repetitive structure that results in a unique periodical saw-tooth pattern in force-extension recordings (Figure 1 B). This "fingerprint" clearly provides the possibility to monitor the unfolding of domains from a single polyprotein, and enables the measurement of the force required to unfold those domains, while giving precise information about their size. For all these reasons, increasing attention has been devoted in the last years toward the design and realization of polyprotein constructs for SMFS in order to investigate proteins involved in amyloidogenic pathologies such as Parkinson's Disease (PD).[5,6] By this approach, it was possible to characterize the conformational diversity of alpha-synuclein and its mutational variants and to observe that, in several unrelated conditions linked to the pathogenicity of PD, their monomeric conformational equilibria shift towards aggregation-triggering β-structured conformers.

In this frame, we focused on β_2-microglobulin (β_2m), an amyloidogenic protein involved in the human disorder dialysis-related amyloidosis (DRA).[7,8] We show the recombinant production of a novel chimeric polyprotein containing the β_2m, flanked on both sides by three tandem repeats titin (I27) modules ($I27_3$–β_2m–$I27_3$), along with its structural investigation, at the single-molecule level, by SMFS. We explored both the wild-type form of β_2m (wt β_2m) and its variant, devoid of N-terminal hexapeptide (ΔN6 β_2m).

Native β_2m is a 99-residues protein with a seven-stranded β-sandwich fold, typical of the immunoglobulin superfamily; it contains two β-sheets that are held together by a single disulphide bond linking Cys25 and Cys80.[9] In vivo, β_2m is present as the non-polymorphic light chain of the class-I major histocompatibility complex (MHC-I). As part of its normal catabolic cycle, β_2m dissociates from the MHC-I complex and is transported in the serum to the kidneys, where the majority (95%) is degraded. Renal failure disrupts the clearance of β_2m from the serum, resulting in an increase of its concentration up to 60-fold. Then, by a mechanism that is currently not well understood, β_2m self-associates into amyloid fibrils that typically accumulate in the musculoskeletal system.[7] To date, several in vitro studies, focusing on the molecular processes that prime β_2m fibrils formation, have demonstrated that, under denaturing conditions (e.g. acidic pH, high ionic strength, fluorinated solvents, etc.),[10,11] as well as in the presence of bivalent ions,[12] wt β_2m acquires a significant tendency to aggregate, possibly due to the increasing concentration of amyloid precursors, such as partially folded monomers or aggregates.[10,13,14] Remarkably, bulk spectroscopic studies revealed that the deletion of the 6 N-terminal residues strongly destabilizes the β_2m native form. Such deleted variant[15] characterized by a lower stability around specific protein strands, is less folded, thus enabling fibrillogenesis even at physiological conditions, without requiring any denaturing stress.[16,17] Moreover, while C, D, E and F β-sheet strands seem to play an important role for the formation of cross-β structure in amyloids,[13] the fraying of the N- and C-terminal strands[18–20] and, thus, their dissociation from the β_2m core, are likely to be deeply involved in amyloids initiation. In this context, it would be of crucial importance to develop new investigation tools, sensitive to the single-molecule level, which may help to better understand the complex structural mechanisms underlying the generation of amyloid deposits. In particular, the opportunity to disclose the specific intramolecular forces involved in the folding stability of β_2m and its deleted variant, at single-molecule level, may be fundamental to identify the structural properties of specific protein domains.

To stretch an individual β_2m molecule by using the atomic force microscopy (AFM) tip, we followed the design proposed by Fernandez et al. for the study of the random coil titin N2B segment[21] employed also for the study of alpha-synuclein.[5,6] We have chosen I27 domains as handles since they introduce well-characterized fingerprint signals into the recorded force curves, making the identification of the unfolding signals of β_2m more clear (Figure 1 B).[22] The chimeric gene encoding the $I27_3$–β_2m–$I27_3$ polyprotein, consisting of a single β_2m module flanked on both sides by three tandem I27 domains, was cloned into the pAFM–β_2m plasmid starting from the pAFM1-4 and pAFM5-8 plasmids (see the Experimental Section).[23] A His–tag and a Cys–Cys tail were inserted at the N- and C-termini of the $I27_3$–β_2m–$I27_3$ polyprotein to facilitate its purification, and covalent attachment to gold surfaces, respectively (Figure 2 A). The construct was designed so that we are sure to have mechanically stretched the β_2m module by AFM, only if in the same curve the number of unfolding signals coming from I27 modules is equal or higher than four[1,24] (Figures 1 and 2 A). By this procedure, we can recognize, in a very stringent way, the signal of the β_2m moiety in each chimeric protein that has been stretched.

The recombinant $I27_3$–β_2m–$I27_3$ polyprotein was first characterized by means of sodium dodecyl sulfate–polyacrylamide gel electrophoresis (SDS-PAGE) and western blot analysis (Figure 2 B). We found that the polyprotein had a purity higher than 97%; the observed electrophoretic mobility was in good agreement with its molecular mass (75 867 Da, calculated with the Protparam software, www.expasy.org). The western blotting analysis also revealed, with high specificity and sensitivity, the presence of β_2m protein in the construct (Figure 2 B).

A further characterization of the recombinant polyprotein was performed by tryptophan (Trp) fluorescence experiments because this technique is a very sensitive probe of protein conformational state. The assessment of the fold pattern of the individual protein modules in the construct, particularly of β_2m, is of great importance, because it is crucial to guarantee that the SMFS experiments are carried out onto a protein that is properly folded. We thus collected fluorescence spectra of the recombinant construct (both in native and denatured conditions) as well as of the two individual constituents of the construct, namely, wild-type β_2m and $I27_6$. The fluorescence spectrum of the $I27_3$–β_2m–$I27_3$ polyprotein was characterized by a broadband emission peaking around 316 nm (Figure 3, top). Under identical conditions, monomeric wt β_2m exhibited a weaker fluorescence spectrum with a maximum (λ_{max}) near 331 nm, while the $I27_6$ revealed a more intense "blue" emission

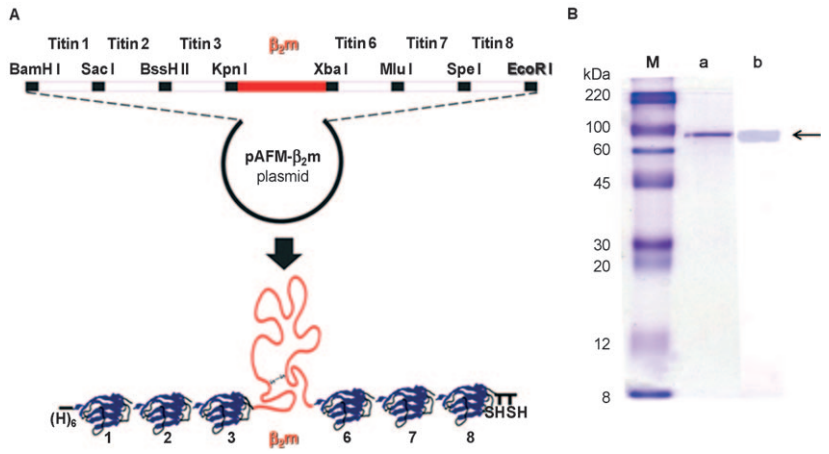

Figure 2. Protein engineering and characterization. A) Schematic diagram of the pAFM–wtβ_2m vector obtained from the cloning of β_2m sequence in pAFM8-m (see the Experimental Section) and representation of the chimeric polyprotein $I27_3$–wt β_2m–$I27_3$. The numbers associated with the titin modules refer to the original vector described by Steward et al.[23] The C-terminal of the polyprotein presents two Cys residues to promote a covalent and specific tethering onto gold surfaces, while the N-terminal has a His-tag for purification. B) SDS-10% PAGE and Western blot analyses of the chimeric polyprotein [M: molecular marker ColorBurst (Sigma, USA); lane a: final product of size-exclusion chromatography; lane b: Western blotting analysis with anti-β_2m antibody; the arrow indicates the band corresponding to $I27_3$–wt β_2m–$I27_3$].

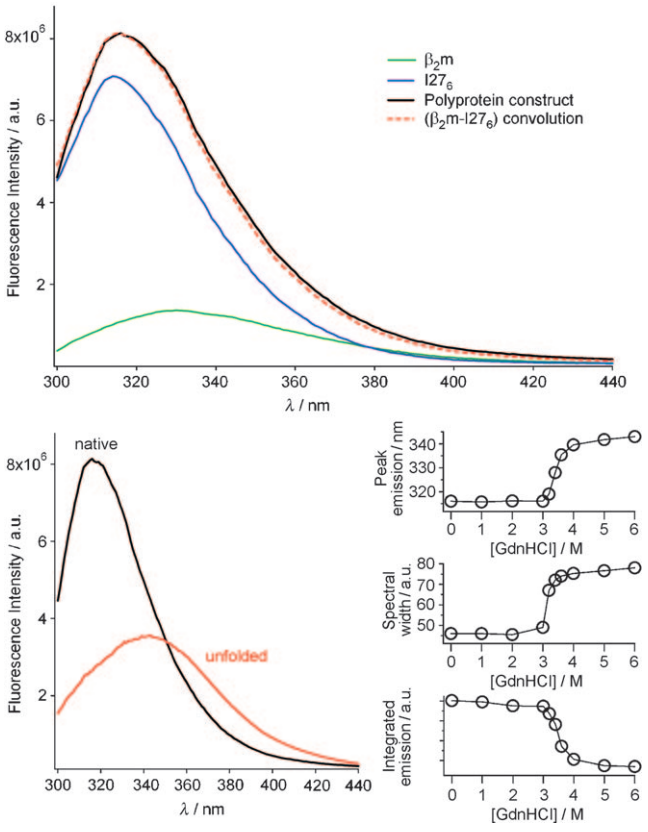

Figure 3. Fluorescence characterization of the recombinant polyprotein. Top: Emission spectrum of the $I27_3$–wt β_2m–$I27_3$ construct as compared to the emission bands of wild-type β_2m and $I27_6$ modules and of their convolution. Bottom (left): Fluorescence spectra of the polyprotein under native and denatured conditions (6 M GdnHCl). Bottom (right): Unfolding transition analyzed by monitoring λ_{max}, spectral width, and integrated emission as a function of the GdnHCl concentration (0–6 M).

with a λ_{max} around 314 nm (Figure 3, top). This latter fluorescence pattern is in good agreement with the emission spectrum of monomeric titin, due to the buried Trp34 residue, meaning that the I27 modules are properly folded within the recombinant construct.[25] Interestingly, the convolution of the emission bands of the native β_2m and of $I27_6$ results in a spectrum that is almost identical to that experimentally observed for the polyprotein (Figure 3, top). Such matching suggests that the β_2m protein, when inserted in the construct, maintains a native-like fold pattern, with no significant perturbations of its conformational features induced by the I27 neighboring domains.[26] The chimeric $I27_3$–β_2m–$I27_3$ polyprotein was, therefore, clearly demonstrated to be suitable for SMFS studies. We further characterized the novel recombinant construct by investigating its unfolding properties upon addition of the classical denaturant guanidinium chloride (Gdn–HCl). The presence of high concentrations of Gdn–HCl resulted in a significant red-shift of its fluorescence spectrum (Figure 3, bottom-left), with λ_{max} reaching a peak around 343 nm, with a consistent broadening of the emission band, accounting for the increased conformational heterogeneity of the protein modules. The polyprotein showed a quite sharp unfolding transition occurring at 3–4 M of Gdn-HCl (Figure 3, bottom, right), as clearly revealed by the three spectral parameters characterizing the conformational state of the protein (i.e. λ_{max}, spectral width, integrated emission).

After conformational assessment of the recombinant polyprotein construct by fluorescence experiments, the $I27_3$–β_2m–$I27_3$ molecules were immobilized onto a flat gold surface under phosphate buffered saline (PBS) conditions and stretched according to the SMFS methodology. Tens of thousands of force vs. extension curves were typically recorded in each experiment. We selected only traces with four, five or six equally spaced I27 unfolding peaks prior to detachment because only in that case we are sure of the presence of the unfolding signal of β_2m (a representative image of the I27 fingerprint composed of five unfolding peaks is reported in Figure 4A). A typical AFM topographical characterization of the $I27_3$–β_2m–$I27_3$ polyprotein is shown in Figure 4B, revealing a quite homogenous globular pattern, with features in the ≈20–30 nm size range and ≈8–10 nm height (likely corresponding to single polyprotein constructs).

The experimental SMFS curves showed regularly spaced peaks characterized by unfolding forces of 150–250 pN, consistent with the unfolding of the I27 module[27] (Figure 4A,

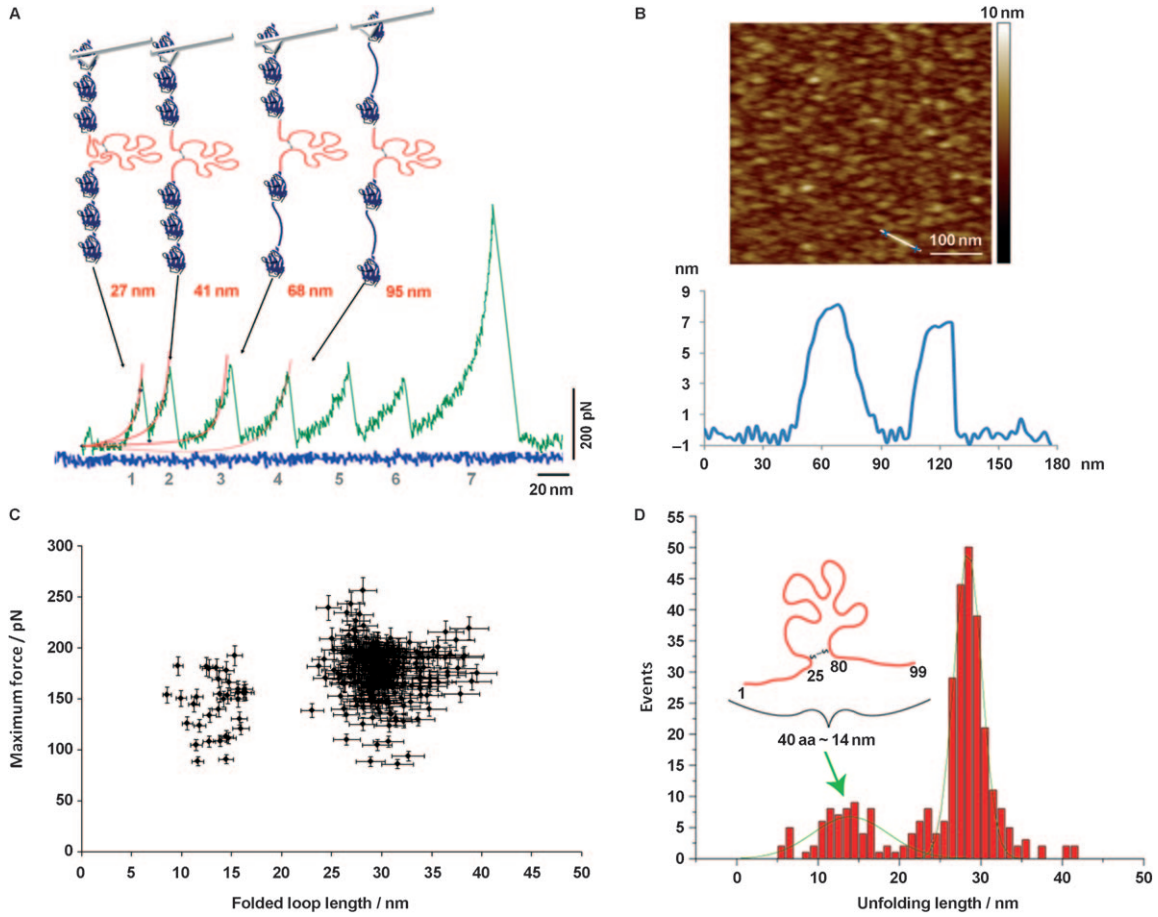

Figure 4. SMFS experiments on the $I27_3$–wt β_2m–$I27_3$ polyprotein. A) A typical force versus distance curve in which the peaks 2–6 represent the unfolding events of single I27 modules (the last peak corresponds to the detachment of the polyprotein molecule). Peak 1 represents the unfolding of a specific portion of β_2m, external to disulfide bridge. The red lines represent the WLC fitting. B) Topographical characterization of the polyprotein construct immobilized onto gold substrates in PBS buffer. C) Unfolding force versus unfolding length plot [(146 ± 27) pN and (14 ± 5) nm; errors were measured as standard deviation]. D) Statistical analysis of the unfolding length recorded in 20 independent experiments after WLC fitting.

peaks 2–6), and a peak near the adhesion point generated by the unfolding of β_2m moiety (Figure 4A, peak 1). By a worm-like chain (WLC) fitting of the peak 1 (see Experimental Section), we obtained an average contour length of 27 nm, corresponding to the extension of five I27 modules in globular conformation (4.5 nm × 5 = 22.5 nm, where 4.5 nm is the dimension of a single I27 module[21]) plus one β_2m protein (22.5 nm + 4.5 nm = 27 nm, where 4.0–4.5 nm is the β_2m size, as determined by dynamic light scattering measurements, data not shown). Notably, also SMFS curves confirmed the correct conformation of the individual protein modules in the recombinant construct. The fitting of peak 2 showed an average contour length of 41 nm (Figure 4A), which can be ascribed to the extension of a mechanically unfolded region of β_2m, external to the disulfide bridge, of 43 amino acids in length [0.33 nm × 43 = 14 nm, where 0.33 nm is the average dimension of an amino acid;[28] 27 nm (peak 1) + 14 nm (peak 2) = 41 nm]. Interestingly, the unfolding force of the peak 1 is (146 ± 27) pN, which indicates that such β_2m region is likely to be characterized by a β-sandwich structure in its folded state, also in line with the typical force values observed for the other β-structures of I27 modules (Figure 4C). Consistently, the fitting of peaks 3 and 4 showed contour lengths of 68 and 95 nm, respectively (Figure 4A), corresponding to the subsequent unfolding of two I27 modules [41 nm (peak 2) + 27 nm = 68 nm, where 27 nm is the typical extension of an unfolded I27 protein, and 68 nm (peak 3) + 27 nm = 95 nm].[21,22,27] The statistical distribution of the unfolding length recorded in all the experiments (ca. 20 independent experiments), after worm-like chain fitting, showed two representative populations of the unfolding peak (Figure 4D): one population can be ascribed to the unfolding events of the reference I27 module (centered around 27 ± 2 nm), while the second (at 14 ± 5 nm) corresponds to an unfolding length of 43 amino acids, associated to the unfolding of a specific region of wt β_2m, namely the N- and C-terminal domains external to the disulfide bridge of the protein.

The possibility to probe with high precision and reliability, at the single-molecule level, the structural features of terminal regions of the β_2m protein, which maintains a native-like fold pattern in the polyprotein construct, prompted us to investigate, by means of SMFS, the structural modification of such regions induced by the removal of the 6 N-terminal residues. We thus produced a polyprotein construct containing the deleted

variant ΔN6 β_2m. Such variant, as also mentioned above, presents an alteration of the tertiary structure that results in a remarkably higher propensity to self-assemble in fibrillar structures, as compared to the full-length form, and is of particular interest since it was isolated from *ex-vivo* fibrils.[15,16]

SMFS experiments on the $I27_3$–ΔN6 β_2m–$I27_3$ polyprotein revealed force versus extension curves with unfolding events corresponding to the typical fingerprint of I27 modules (Figure 5A, peaks 2–7) along with the ΔN6 variant (Figure 5A, peak 1, and Figure 5B). Noteworthy, unlike the protein construct containing the full length β_2m, the WLC fitting of peak 1 shows different values of unfolding force and unfolding contour length (Figures 5C and 5D). In particular, we found out an unfolding force of 80 pN ± 17 pN, revealing that the protein domains external to the disulfide bridge in the ΔN6 variant are organized in random coil structure, and not in β-structures like in the wild type protein.[21,22,27] Such a result was also confirmed by the statistical analysis of the distribution of the unfolding contour length, which was found to be (11.5 ± 3) nm, that is, equivalent to the 34 a.a. external to the disulfide bridge of ΔN6 β_2m (Figure 5D). The SMFS technique allowed us, therefore, to directly observe, at the single molecule level, the destabilization of the terminal regions in the ΔN6 variant. This finding is of crucial importance because such a characteristic is mostly responsible for the higher tendency of ΔN6 to form amyloid fibrils.

In conclusion, by means of SMFS, we have described the structural differences of the terminal strands (which have a key role in the fibrillogenesis) of wt β_2m and its truncated variant ΔN6 β_2m, presenting a higher amyloidogenic potential. In principle, such innovative tools may open interesting perspective to develop tailored strategies to treat misfolding diseases, thanks to their advantages over bulk "averaged" methodologies, including the potential to accurately detect and quantify poorly represented conformer distributions of β_2m. Notably, the insertion of stabilizing or destabilizing amino acids in controlled regions of genetically engineered β_2m variants, by site-specific mutagenesis, may provide, in combination with SMFS technique, a novel tool to explore the intricate mechanisms underlying the misfolding processes of the protein, along with the initial formation of aggregates. Moreover, the possibility to perform the experiments in the liquid phase provides an attractive chance to investigate the protein in a physiological environment, or under controlled conditions which are known to prime or inhibit the fibrillogenesis, such as the presence of

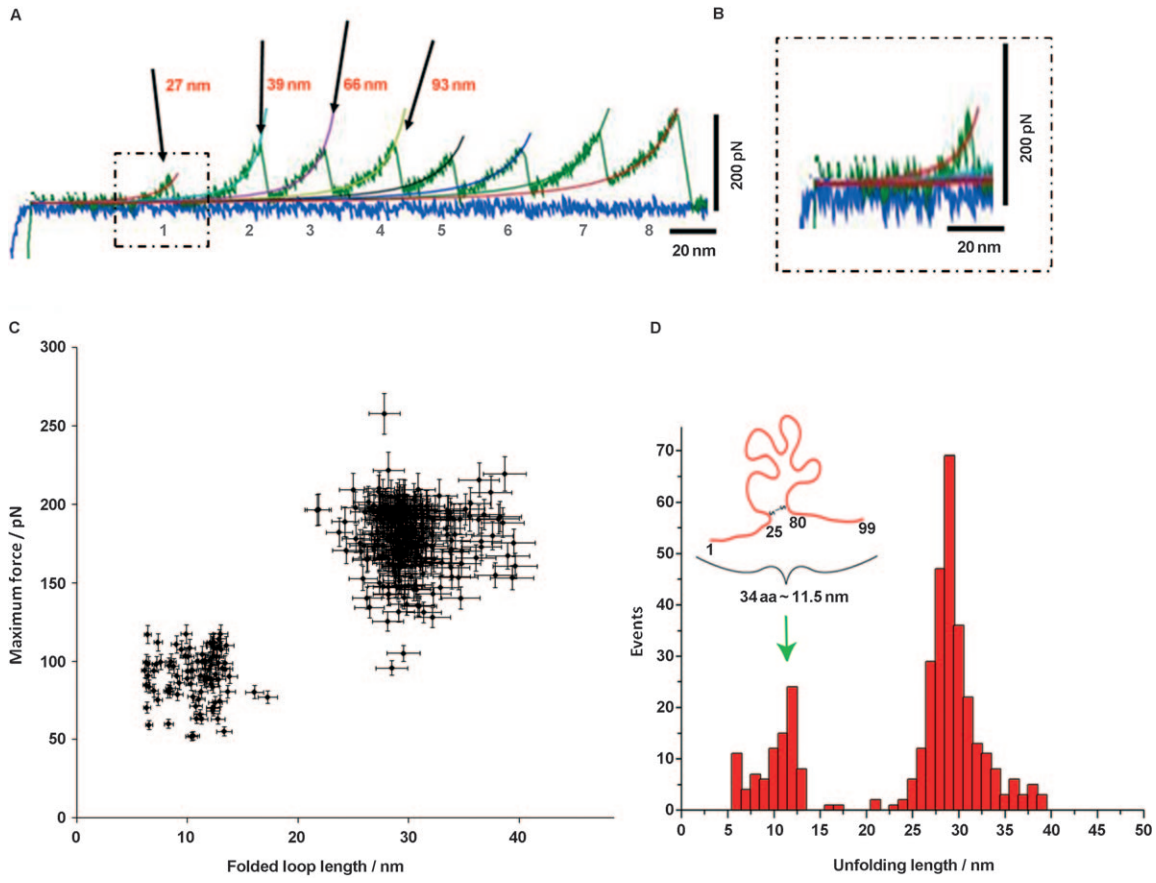

Figure 5. SMFS experiments on the $I27_3$–ΔN6 β_2m–$I27_3$ polyprotein. A) A typical force versus distance curve in which peaks 2–7 represent the unfolding events of single I27 modules (the last peak corresponds to the detachment of the polyprotein molecule). Peak 1 shows different unfolding force and unfolding length of the specific domains of ΔN6 β_2m, thereby revealing the region of 34 residues, external to the disulfide bridge, structured in a random-coil. B) The panel shows a zoom of the region enclosed by the dashed squares. C) Unfolding force versus unfolding length plot [(80 ± 17) pN and (11.5 ± 3.0) nm; errors were measured as standard deviation]. D) Statistical analysis of the unfolding length recorded in 30 independent experiments after WLC fitting.

Cu^{2+}, preformed seeds, ligands, organic solvents, and/or different pH values.

Experimental Section

Polyprotein Design and Expression: Chimeric genes encoding the $I27_3$–wt β_2m–$I27_3$ and $I27_3$–ΔN6 β_2m–$I27_3$ polyproteins were obtained starting from pAFM1-4 and pAFM5-8 plasmids, kindly provided by J. Clarke (Cambridge University, UK), and constructed according to Steward et al.[23] These plasmids were used to obtain a vector with eight I27 modules, named pAFM8-m. β_2m cDNA was amplified by PCR using a pair of primers containing *KpnI* and *XbaI* sites and the pβ_2m template, kindly provided by F. Calabi (NNL, Lecce). To substitute the two central titin modules of pAFM8-m, the pAFM8-m plasmid was then digested with *KpnI* and *XbaI* and ligated to the amplified β_2m sequence, to give the final pAFM-wt β_2m and pAFM-ΔN6 β_2m vectors. Therefore, the obtained expression plasmids encode chimeric polyproteins composed of a single wild-type β_2m or a variant ΔN6 module, flanked on both sides by three tandem I27 domains. The pAFM-wt β_2m and pAFM-ΔN6 β_2m vectors were used to transform *E. coli* BL21(DE3) cells (Stratagene, La Jolla, CA). The expression of the recombinant protein was induced as described by Steward et al.[23] The recombinant protein was purified by Ni^{2+} affinity chromatography (His-Select Cartridge, Sigma) starting from *E. coli* crude protein extract equilibrated in 50 mM sodium phosphate buffer pH 7.4, 300 mM NaCl, 20 mM imidazole. The bound proteins were eluted from the resin with 250 mM imidazole. The recombinant polyprotein was further purified by size-exclusion chromatography (Superdex 200 10/300 GL, Amersham Bioscences) with 50 mM sodium phosphate buffer pH 7.4, 300 mM NaCl and desalted-concentrated by Amicon Ultra-15 (Millipore, USA). Western blot analysis was carried out using an anti-β_2m Ab BBM.1 (Santa Cruz Biot, USA) and visualized with BCIP/NBT alkaline phosphatase substrate kit (Vector Lab., USA). The recombinant polyproteins exhibit a purity higher than 97%, as probed by 10% SDS-PAGE and size-exclusion chromatography (not mentioned in the text). The polyproteins were finally stored as lyophilized powders.

The $I27_6$ was obtained by cloning two I27 modules in the *NheI* and *EcoRI* sites of pAFM1-4. The two I27 modules were amplified by PCR (introducing the *NheI* and *XbaI* restriction sites for the first module and *XbaI* and *EcoRI* for the second module) and subsequently self-ligated. The $I27_6$ multimodular protein was expressed into *E. coli* BL21(DE3) (Stratagene, La Jolla, CA) and purified by Ni^{2+} affinity chromatography (His-Select Cartridge, Sigma) and size-exclusion chromatography (Superdex 200 10/300 GL, Amersham Bioscences). The purity was checked by 7.5% SDS-PAGE and high-performance liquid chromatography (HPLC) and found to be higher than 95% (data not shown).

Wild-type β_2m protein (purity higher than 95%) was purchased from BD Biosciences (NJ, USA).

Trp Fluorescence Measurements: Trp fluorescence spectra were recorded in the photon-counting mode by using a 450 W xenon lamp as the source of excitation and double monochromators both in excitation and emission. The emitted light was collected at right angles to the excitation radiation. Photoluminescence spectra of control samples were always recorded and subtracted from the experimental samples to correct for background. All the experiments were performed at room temperature (20 °C) with typical protein concentrations of 0.6 μM; the excitation wavelength was 280 nm (2 nm bandwidth) while the emission (2 nm bandwidth) was collected from 300 to 440 nm. Unfolding experiments of the $I27_3$–wt β_2m–$I27_3$ construct were performed in the 0–6 M concentration range of Gdn-HCl.

Atomic Force Microscopy Imaging: The polyprotein, immobilized onto gold substrates, was characterized under fluid conditions by a Nanoscope IV MultiMode SPM (Veeco Instruments, Santa Barbara, CA). Ultrasharp silicon cantilevers RTESPA (Veeco Instruments, Santa Barbara, CA) were used with a typical resonance frequency of 250 kHz. The images were analyzed by using the NanoScope software (Digital Instruments, version 6.0).

SMFS Experiments: For each experiment, a 20 μL drop of polyprotein solution (100 $\mu g\,mL^{-1}$) was deposited onto a freshly peeled gold surface for about 20 min. SFMS experiments were performed by means of a Picoforce AFM with a Nanoscoope IIIa controller (Digital Instruments) using V-shaped silicon nitride cantilevers (NP, Digital Instruments) with a spring constant calibrated by thermal noise method.[29] The pulling speed was 2.18 $\mu m\,s^{-1}$ for all experiments. The buffer was 10 mM PBS. The force curves were analyzed using the commercially available software from Digital Instrument (Nanoscope v6.12r2) and Hooke, a Python-based home-coded force spectroscopy data analysis program available at http://code.google.com/p/hooke/. Force curves were analyzed fitting each peak with a worm-like chain (WLC) force versus extension model[30] having the following equation [Eq. (1)]:

$$F = \left(\frac{k_b T}{p}\right)\left[\frac{1}{4\left(1-\frac{x}{L_0}\right)^2} - \frac{1}{4} + \frac{x}{L_0}\right] \quad (1)$$

By applying this model, it is possible to obtain properties such as the contour length (L_0) and the persistence length (p). The I27 reference modules were characterized in terms of L_0 after each unfolding event.

Acknowledgements

The authors gratefully acknowledge J. Clarke (Cambridge University, UK) for kindly providing the vectors for construct expression, F. Calabi for kindly providing the pβ_2m plasmid, F. Valle, L. L. del Mercato, G. Maiorano, and R. Chiuri for useful discussions and for help during experiments, and V. Fiorelli for the expert technical assistance. This work was supported by the Italian Ministry of Research through MIUR "FIRB" projects (RBLA03ER38_001 and RBNE03FMCJ_003).

Keywords: β_2-microglobulin · dialysis-related amyloidosis · fluorescence spectroscopy · proteins · single-molecule studies

[1] R. Perez-Jimenez, S. Garcia-Manyes, S. R. Ainavarapu, J. M. Fernandez, *J. Biol. Chem.* **2006**, *281*, 40010–40014.
[2] D. Sharma, O. Perisic, Q. Peng, Y. Cao, C. Lam, H. Lu, H. Li, *Proc. Natl. Acad. Sci. USA* **2007**, *104*, 9278–9283.
[3] T. E. Fisher, M. Carrion-Vazquez, A. F. Oberhauser, H. Li, P. E. Marszalek, J. M. Fernandez, *Neuron* **2000**, *27*, 435–446.
[4] M. Carrion-Vazquez, A. F. Oberhauser, S. B. Fowler, P. E. Marszalek, S. E. Broedel, J. Clarke, J. M. Fernandez, *Proc. Natl. Acad. Sci. USA* **1999**, *96*, 3694–3699.
[5] M. Sandal, F. Valle, I. Tessari, S. Mammi, E. Bergantino, F. Musiani, M. Brucale, L. Bubacco, B. Samorì, *Plos Biology* **2008**, *6*, 99–108.
[6] M. Brucale, M. Sandal, S. Di Maio, A. Rampioni, I. Tessari, L. Tosatto, M. Bisaglia, L. Bubacco, B. Samorì, *ChemBioChem* **2009**, *10*, 176–83.

[7] J. Floege, M. Ketteler, *Kidney Int.* **2001**, *59*, S164–S171.
[8] J. D. Sipe, *Amyloid Proteins. The Beta-Sheet Conformation and Disease Vol I*, Wiley-VCH, **2005**.
[9] C. H. Trinh, D. P. Smith, A. P. Kalverda, S. E. Phillips, S. E. Radford, *Proc. Natl. Acad. Sci. USA* **2002**, *99*, 9771–9776.
[10] V. J. McParland, N. M. Kad, A. P. Kalverda, A. Brown, P. Kirwin-Jones, M. G. Hunter, M. Sunde, S. E. Radford, *Biochemistry* **2000**, *39*, 8735–8746.
[11] K. Yamaguchi, H. Naiki, Y. Goto, *J. Mol. Biol.* **2006**, *363*, 279–288.
[12] C. J. Morgan, M. Gelfand, C. Atreya, A. D. Miranker, *J. Mol. Biol.* **2001**, *309*, 339–345.
[13] V. J. McParland, A. P. Kalverda, S. W. Homans, S. E. Radford, *Nat. Struct. Biol.* **2002**, *9*, 326–331.
[14] F. Chiti, E. De Lorenzi, S. Grossi, P. Mangione, S. Giorgetti, G. Caccialanza, C. M. Dobson, G. Merlini, G. Ramponi, V. Bellotti, *J. Biol. Chem.* **2001**, *276*, 46714–46721.
[15] V. Bellotti, M. Stoppini, P. Mangione, M. Sunde, C. Robinson, L. Asti, D. Brancaccio, G. Ferri, *Eur. J. Biochem.* **1998**, *258*, 61–67.
[16] G. Esposito, R. Michelutti, G. Verdone, P. Viglino, H. Hernández, C. V. Robinson, A. Amoresano, F. Dal Piaz, M. Monti, P. Pucci, P. Mangione, M. Stoppini, G. Merlini, G. Ferri, V. Bellotti, *Protein Sci.* **2000**, *9*, 831–845.
[17] G. Esposito, A. Corazza, P. Viglino, G. Verdone, F. Pettirossi, F. Fogolari, A. Makek, S. Giorgetti, P. Mangione, M. Stoppini, V. Bellotti, *Biochim. Biophys. Acta* **2005**, *1753*, 76–84.
[18] S. Jones, D. P. Smith, S. E. Radford, *J. Mol. Biol.* **2003**, *330*, 935–941.
[19] J. Kim, Y. Motomiya, M. Ueda, M. Nakamura, Y. Misumi, S. Saito, S. Ikemizu, S. Misumi, K. Ota, S. Shinriki, H. Kai, Y. Ando, *Ann. Clin. Biochem.* **2008**, *45*, 489–495.
[20] G. Esposito, S. Ricagno, A. Corazza, E. Rennella, D. Gümral, M. C. Mimmi, E. Betto, C. E. Pucillo, F. Fogolari, P. Viglino, S. Raimondi, S. Giorgetti, B. Bolognesi, G. Merlini, M. Stoppini, M. Bolognesi, V. Bellotti, *J. Mol. Biol.* **2008**, *378*, 887–897.
[21] H. Li, W. A. Linke, A. F. Oberhauser, M. Carrion-Vazquez, J. G. Kerkvliet, H. Lu, P. E. Marszalek, J. M. Fernandez, *Nature* **2002**, *418*, 998–1002.
[22] M. C. Carrion-Vazquez, A. F. Oberhauser, T. E. Fisher, P. E. Marszalek, H. Li, J. M. Fernandez, *Prog. Biophys. Mol. Biol.* **2000**, *74*, 63–91.
[23] A. Steward, J. L. Toca-Herrera, J. Clarke, *Protein Sci.* **2002**, *11*, 2179–2183.
[24] R. B. Best, B. Li, A. Steward, V. Daggett, J. Clarke, *Biophys J.* **2001**, *81*, 2344–2356.
[25] A. S. Politou, D. J. Thomas, A. Pastore, *Biophys J.* **1995**, *69*, 2601–2610.
[26] S. Batey, J. Clarke, *J. Mol. Biol.* **2008**, *378*, 297–301.
[27] H. Li, A. F. Oberhauser, S. B. Fowler, J. Clarke, J. M. Fernandez, *Proc. Natl. Acad. Sci. USA* **2000**, *97*, 6527–6531.
[28] A. Sarkar, S. Caamano, J. M. Fernandez, *J. Biol. Chem.* **2005**, *280*, 6261–6264.
[29] E. L. Florin, M. Rief, H. Lehmann, M. Ludwig, C. Dornmair, V. T. Moy, H. E. Gaub, *Biosensors Bioelectron.* **1995**, *10*, 895–901.
[30] C. Bustamante, J. F. Marko, E. D. Siggia, S. Smith, *Science* **1994**, *265*, 1599–1600.

Received: March 20, 2009
Published online on June 3, 2009

